ChemComm
Chemical Communications

This article can be cited before page numbers have been issued, to do this please use: C. E. Ward, R. J. Maguire, N. Kumar, J. D. Badjic and C. M. Hadad, *Chem. Commun.*, 2026, DOI: 10.1039/D6CC02397E.

ROYAL SOCIETY OF CHEMISTRY

rsc.li/chemcomm

ChemComm

View Article Online
DOI: 10.1039/D6CC02397E

COMMUNICATION

Narcissistic Assembly of Homochiral Covalent Organic Cages with Dehydrobenzo[12]Annulene (DBA) Panels

Carson E. Ward,[a] Ryan J. Maguire,[a] Nitesh Kumar,[a] Christopher M. Hadad,[a] and Jovica D. Badjić*[a]

Received 00th January 20xx,
Accepted 00th January 20xx

DOI: 10.1039/x0xx00000x

Dynamic imine condensations of a trivalent dehydrobenzo[12]annulene (DBA) with (1*R*,2*R*)- or (1*S*,2*S*)-cyclohexane-1,2-diamine (*R*/*S*-CDA) yield homochiral [2+3] organic cages through narcissistic self-sorting. This study represents the first successful incorporation of multiple dehydrobenzoannulenes into discrete and chiral supramolecular structures for potential application in catalysis, molecular storage, and optoelectronics.

Shape-persistent organic cages[1] (Figure 1) are rigid, symmetric, and often hollow molecules assembled in a single reaction step using principles of dynamic covalent chemistry.[2] After two (or more) building units are subjected to reversible formation/breakage of covalent bonds (i.e., imine, boronate, disulfide, etc.),[3] discrete covalent cages may form as the primary thermodynamic product;[4] they are labeled [n+m], with n and m corresponding to the number of comprising units. Indeed, the notion of a rapid and efficient construction of sizeable, yet hollow, organic capsules in high yield[5] has been of great interest to supramolecular chemists.[6] So far, the cages have been probed for gas capture/storage,[7] sequestration of drugs,[8] anion recognition,[9] catalysis,[10] and separation.[11] Interestingly, predicting the outcome of dynamic covalent processes for obtaining targeted structures is still a challenging task with solvent,[12] temperature,[13] template,[9a] and shape of molecular building blocks[14] playing a role. For example, reversible imine-condensation of (1*R*,2*R*)-cyclohexane-1,2-diamine (*R*-CDA) and 1,3,5-triformylbenzene gave [4+6] cage (Figure 1A) as the major product.[15] On the other side, the condensation of *R*-CDA with 1,3,5-triformylphloroglucinol yielded[16] [2+3] cage (Figure 1A) despite the notion that trivalent 1,3,5-triformylbenzene and 1,3,5-triformylphloroglucinol are almost identical in size and shape. While Cooper and coworkers reported[17] that the number of carbon atoms (i.e., odd or even), separating two amino groups within diamino building blocks, could determine [2+3] versus [4+6] condensation outcome, there is clearly more to the phenomenon. On that note, we wondered: would the imine condensation of dehydrobenzo[12]annulene **2** (DBA **2**, Figure 1B)[18] and *R*-CDA give rise to tetrahedral [4+6] (**3**, Figure 1B) or trigonal [2+3] cage (**1**, Figure 1B)? In this regard, truxene[13] and triazine[19] (Figure 1C) were shown to undergo imine condensation with *R*-CDA and give [4+6] cages. With conformational dynamics, radius, and surface area of DBA **2** similar to the studied aromatic systems (Figure 1C), we reasoned that the reaction of DBA **2** with *R*-CDA would likely yield [4+6] cage **3** (Figure 1B). Furthermore, DBA **2** is a C_{3h} symmetric molecule with σ_h plane of symmetry. Upon

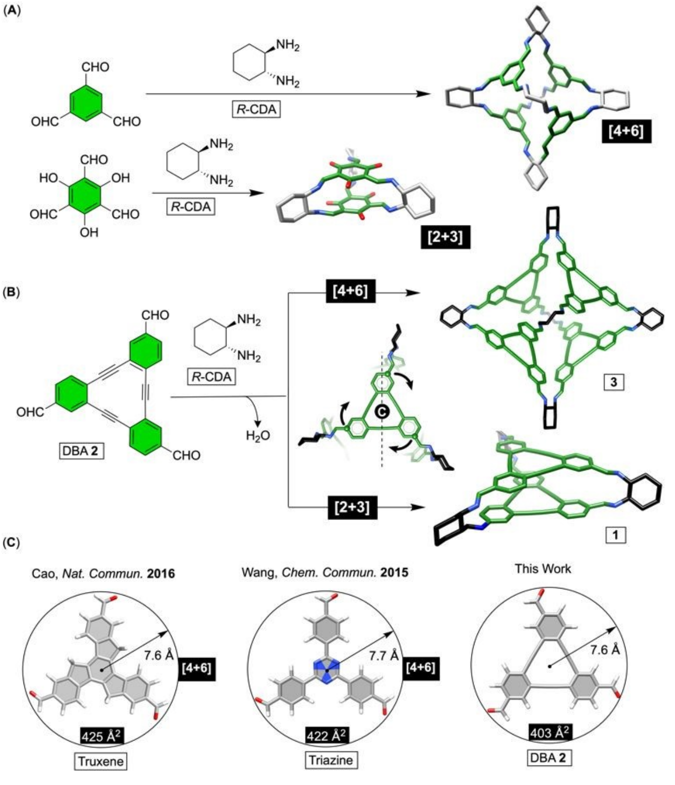

Fig. 1 (A) X-ray structures (see ref. 15a and 16) of [4+6] and [2+3] organic cages obtained by reversible condensations of two benzene derivatives and *R*-CDA. (B) Dynamic imine condensation dehydrobenzo[12]annulene derivative DBA **2** with *R*-CDA could give [4+6] (OPLS 4, Maestro) or [2+3] (OPLS 4, Maestro) cages. (C) Stick representation of energy minimized (PM3, Spartan) truxene, triazene and DBA **2**.

---

[a] *Department of Chemistry & Biochemistry, The Ohio State University, Columbus (OH) 43210 USA*
† C. E. Ward, R. J. Maguire, N. Kumar, Prof. C. M. Hadad, Prof. J. D. Badjić

View Article Online
DOI: 10.1039/D6CC02397E

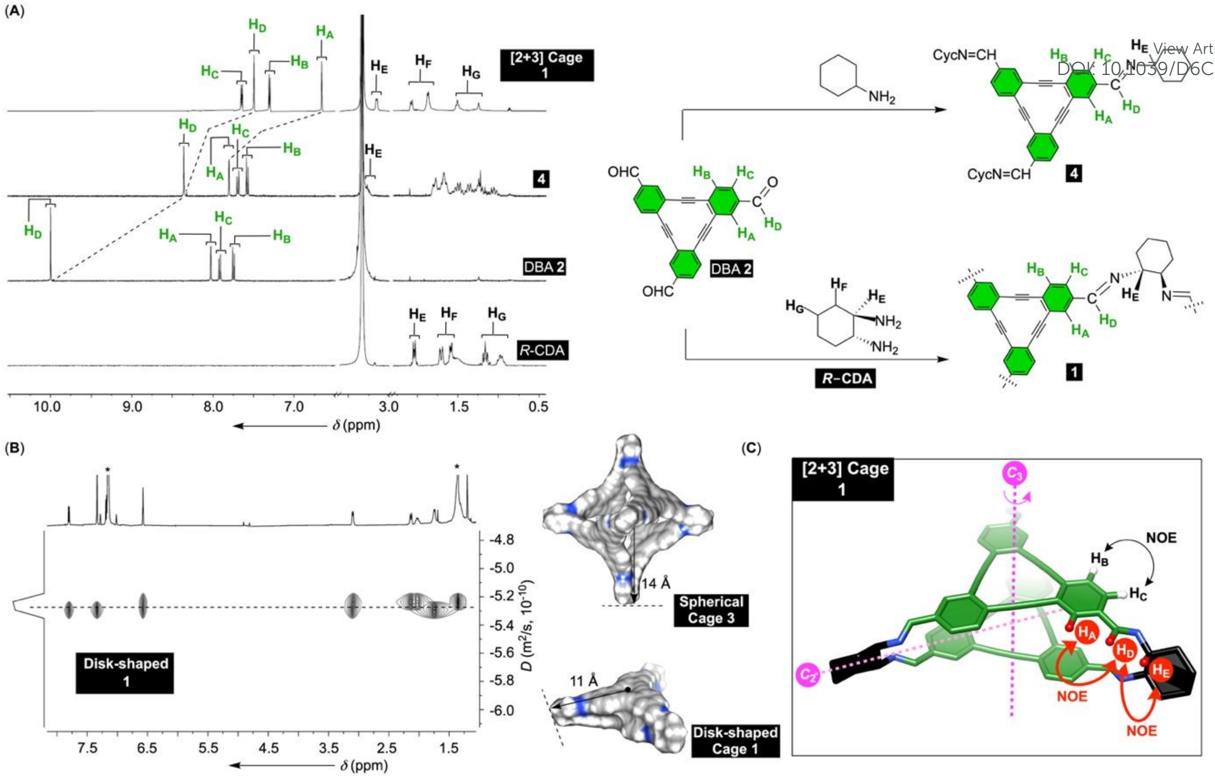

Fig. 2 (A) ^{1}H NMR spectra (600 MHz, 298 K) of *R*-CDA, DBA **2**, model *tris*-imine **4** and [2+3] cage **1** in DMSO-d_6. (Right) Chemical structures of **1** and **4** along with their preparation from DBA **2**. (B) ^{1}H NMR DOSY spectrum (600 MHz, 298 K) of cage **1** in C_6D_6. (Right) van der Waals surfaces of [4+6] cage **3** and [2+3] cage **1**. (C) Ball and stick representation of cage **1** showing its elements of symmetry in addition to experimentally observed NOE cross signals (Figure S15).

its incorporation into cage **3** (or **1**), it loses σ_h element of symmetry with four DBA panels assuming clockwise (C, Figure 1B), counterclockwise (A) or both C and A orientations.[13] As for C_{3h} truxene (Figure 1C), the reaction with *R*-CDA was stereoselective,[13] leading to the formation of homochiral [4+6] product with all four truxenes assuming anticlockwise (*A*) orientation. Will we observe chirality transfer and stereoselectivity in dynamic covalent synthesis of cages **1** or **3** (Figure 1B)? Furthermore, dynamic imine condensation of a racemic mixture of *R*-CDA and *S*-CDA with truxene led to the sole formation of (*R*)-CDA$_6$(*AAAA*) and *S*-CDA$_6$(*CCCC*) products and no cages having both *R*- and *S*-CDA were incorporated in the framework.[20] The observed stereoselectivity in which only chiral molecules of the same type (i.e., *R*-CDAs with DBAs of *A* orientations) are included in the product is clearly narcissistic self-sorting.[21] On the contrary, D_{3h} symmetric triazine[20] or 1,2,5-triformylbenzene[22] (Figure 1A) reacted with racemic *R*/*S*-CDA to give a mixture of stereoisomeric [4+6] cages including both *R* and *S* cyclohexane enantiomers. This begged the question: how will DBA **2** react with racemic *R*/*S*-CDA? So far, DBA macrocycles[18] have been of a great interest for creating optoelectronic, storage and catalytic materials.[23] In particular, DBAs coordinate Ni(0) using three alkynes to promote catalytic desulfurization of aromatics.[24] Would [4+6] cage **3** with Ni(0) at its panels catalyze desulfurization reactions inside its spacious cavity?

In order to obtain DBA **2**, we slightly modified the reported 9-step synthesis of this compound (Scheme S1A).[25] Next, we used mass spectrometry (Figure S8) to screen the outcome of dynamic imine condensations of *R*-CDA and DBA **2** in six different solvents. In benzene, chloroform, *N*,*N*-dimethylformamide and toluene, there were two signals suggesting the formation of [2+3] and/or [4+6] cages (Figure S8). After, the two reactants were added to benzene (C_6D_6), containing a catalytic quantity of trifluoroacetic acid (TFA), and the condensation was monitored with ^{1}H NMR spectroscopy (Figure S9). A change in the signal appearance over time corroborated reversible imine exchange taking place, and then after 300 min, the process resulted in the formation of a single set of signals: the integration ratio of resonances from two building blocks was 1:1.5 while the newly formed imine C–H$_D$ appeared as singlet at 7.8 ppm (Figure 2A; Figure S10). After isolation of the main product (Scheme S4), we completed high resolution electrospray ionization (ESI) measurements (Figure S12). The data from trapped ion mobility (TIMS) coupled with time-of-flight (TOF-ESI) mass spectrometry revealed the most intense peak corresponding to a singly charged cation at m/z = 1003.4476 Da. The observed ion corresponds to [2+3] condensate (1003.4482 Da) corroborating the exclusive formation of cage **1** from *R*-CDA and DBA **2** (Figure 1B). This certainly came as a surprise since the imine condensation of similarly sized and shaped aromatic systems,[13, 19] such as truxene and triazene (Figure 1C), with *R*-CDA led to the formation of [4+6] products. ^{1}H NMR DOSY of **1** (Figure 2B; Figure S13) showed that all of its signals are part of one molecule moving at identical rate with the diffusion coefficient D = 5.36 · 10^{-10} m^2/s. The radius of energy-minimized and spherical [4+6] cage **3** is r = 1.4 nm while disk-shaped **1** is smaller with r = 1.1 nm (Figure 2B). From the Stokes-Einstein

View Article Online
DOI: 10.1039/D6CC02397E

formula for spherical particles (D = k$_B$·T/6π·η·r), the apparent radius of our cage was from the experimental diffusion coefficient computed to be 0.7 nm therefore smaller than expected for both **1** and **3**. However, using the Stokes-Einstein disk approximation formula (D = k$_B$·T/12π·η·r; omnicalculator.com) gave for the experimental r = 1.1 nm, thereby consistent with the computed size of **1**.

To fully assign ^{1}H NMR resonances from **1** (Figure 2A), we recorded its ^{1}H-^{1}H COSY (Figure S14) and ^{1}H-^{1}H ROESY NMR (Figure S15) spectra. From the cross peaks of *J*-coupled protons, we assigned all of ^{1}H NMR signals in **1**. After ^{1}H NMR spectrum of **1** is compared to DBA **2** and *R*-CDA (Figure 2A), a magnetic shielding of the aromatic H$_A$-H$_C$ resonances is apparent with $\Delta\delta$ = –1.4 ppm for H$_A$ (Figure 2A). Since [2+3] cage **1** must include two DBA aromatics on top of one another, the observed diamagnetic shielding of H$_A$-H$_C$ is in line with the structure. On the other side, two sets of 2D cross-peaks from ^{1}H-^{1}H ROESY (Figure 2C; Figure S15) revealed that H$_E$/H$_D$ and H$_D$/H$_A$ protons are close in space. Accordingly, H$_E$ from the cyclohexane ring was deduced to be in plane with the *trans* imine[16] bond and eclipsed with the imine H$_D$ for reducing the 1,3-allylic strain.[26] In addition, H$_D$ is coplanar with H$_A$ from DBA and thus in its vicinity while H$_B$/H$_C$ stay on the opposite side (Figure 2C). Importantly, the coplanarity of H$_E$/H$_D$/H$_A$ protons can also be seen from X-ray structures of [4+6] cages reported in the literature.[13, 15a, 19]

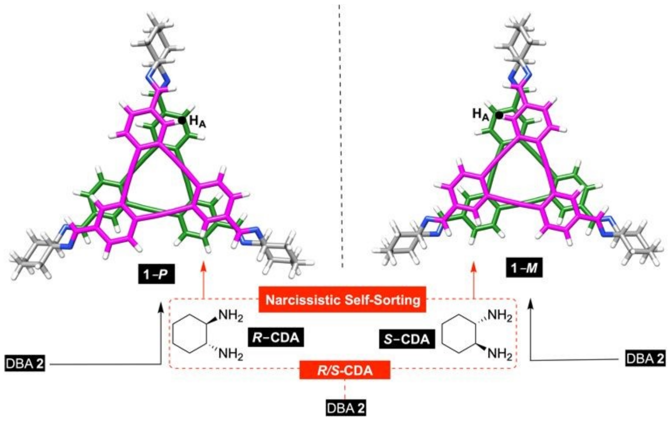

Fig. 3 Stick representations of energy minimized (OPLS 4, Maestro) **1**-*P* and **1**-*M* cages, each with a distinct helical chirality of two stacked DBA rings. Imine condensations of DBA **2** with *R*-CDA, *S*-CDA (black), or racemic *R*/*S*-CDA (red) give **1**-*P*, **1**-*M*, and racemic **1**-*P*/*M* products, respectively.

Furthermore, a single set of ^{1}H NMR resonances from two DBAs and three *R*-CDAs within **1** (Figure 2A) indicated (a) the existence of a C_3 rotation axis for making three *R*-CDAs equivalent (Figure 2C) and (b) three perpendicular C_2 symmetry axis running through each of *R*-CDA groups (Figure 2C) for making top and bottom DBA aromatic rings to be chemically equivalent. With the available structural information, we bult D_3 symmetric **1** *in silico* and after energy-minimization (OPLS4, Figure 3)[17] noted that two aromatic rings are twisted clockwise[16] (C, see also Figure 1B): with the right-handed sense of helical chirality in **1**, we herein label this molecule as **1**–*P*.[27] From the computed structure of **1**-*P*, one can easily note that H$_A$ protons from each DBA reside in diamagnetic shielding area of the opposite macrocycle (Figure 3). This is in line with the large shielding of H$_a$ from **1**-*P* in regard to DBA **2** ($\Delta\delta$ = –1.4 ppm, Figure 2A) and *tris*-imine model compound **4** ($\Delta\delta$ = –1.1 ppm, Figure 2A).

While *R*-CDA directed two DBA units within cage **1** to assume right-handed *P* helicity, we presumed that the condensation of *S*-CDA with DBA **2** ought to give its enantiomer **1**-*M* (Figure 3). Indeed, ^{1}H NMR spectrum the imine product of the latter was equivalent to **1**-*P* (Figure S16). On the other side, using a racemic mixture of *R*-CDA and *S*-CDA in dynamic imine condensation with DBA **2** resulted in the sole formation of **1**-*M* and **1**-*P* cages (Figure 3). The evidence came from ^{1}H NMR spectrum of the isolated product (Figure S16) (a) matching those of **1**-*P*/**1**-*M* molecules and (b) lacking any resonances that would imply the presence of diastereomeric cages. We posit that the narcissistic self-sorting in the formation of homochiral **1**-*P* and/or **1**-*M* is in part arising from intramolecular π–π contacts of stacked DBA rings within each cage (Figure 4C). Indeed, truxene possessing alkyl chains (not shown in Figure 1C) guided the formation of its homochiral [4+6] cage in the narcissistic manner by using intramolecular interactions of these groups.[20] On the contrary, triazene (Figure 1C) and 1,3,5-triformylbenzene (Figure 1A) showed no narcissistic self-sorting in the formation of their [4+6] cages since there was no intramolecular noncovalent contacts between the aromatic panels.[19]

To confirm the computed helical chirality of **1**-*P* and **1**-*M* (Figure 3),[28] we collected their UV-Vis (Figure 4A; Figure S17) and circular dichroism (CD, Figure 4B) spectra. Two broad absorption bands of each homochiral cage at 305 and 310 nm depict electronic transitions within planar and π–conjugated dehydrobenzo[12]annulene aromatics.[29] Concurrently, CD spectra of **1**-*P* and **1**-*M* are the mirror image of one another with three main transitions at 310, 325, and 338 nm: while **1**-*M* shows two bigger positive and one smaller negative Cotton effects, its enantiomer **1**-*P* is the opposite. CD spectrum of the product from racemic *R*/*S*-CDA reacting with DBA **2**, showed no features (pink, Figure 4B) therefore corroborating the presence of racemic **1**-*M*/**1**-*P* which in line with the proposed narcissistic self-sorting operating in the assembly. Next, we went on to compute UV-Vis and CD spectra of **1**-*M* using density functional theory (DFT).[30] Geometry optimization of **1**-*M* was completed at B3LYP-D3/6-31+G* level of theory with the inclusion of D3 dispersion correction[16] to account for van der Walls and aromatic interactions of two DBAs.[31] In this way, the DBAs were found to reside at 3.6 Å distance, thereby forming attractive π–π contacts (Figure 4C; Figure S29).[32] To compute UV-Vis/CD spectra of **1**-*M* (Figure 4A), we used time-dependent[33] DFT method (wB97XD/6-31+G*) with wB97XD functional to account for intramolecular dispersion and noncovalent interactions within the cage.[34] While the computed UV-Vis of **1**-*M* matched the experimental one, the computed CD spectrum predicted all three Cotton effects along with their sign! The left-handed helical chirality within **1**-*M* predicted by ^{1}H NMR spectroscopy in combination with molecular mechanics is thus confirmed by CD spectroscopy and quantum mechanical calculations. A Pinnick oxidation (i.e., imine-to-amide conversion; Scheme S5)[35] of dynamic **1**-*P* and **1**-*M* into robust **5**-*P* and **5**-*M* cages (Figure

View Article Online
DOI: 10.1039/D6CC02397E

4D) was, in each case, an effective process; both **5**-*P* and **5**-*M* were characterized by ^{1}H NMR (Figures S18-S21), mass spectrometry (Figure S22), UV-Vis (Figure S23) and CD spectra (Figure S24). With [3+2] cage **5**-*P*, comprising six stable amide linkages, we attempted its coordination to Ni(0) (Scheme S6).[24] Preliminary results suggested the formation of [Ni(0)$\subset$**5**-*P*] (ESI, Figure S25) although the poor solubility of this product prevented its characterization (with standard methods) and further catalytic studies about which we plan to report in the near future.

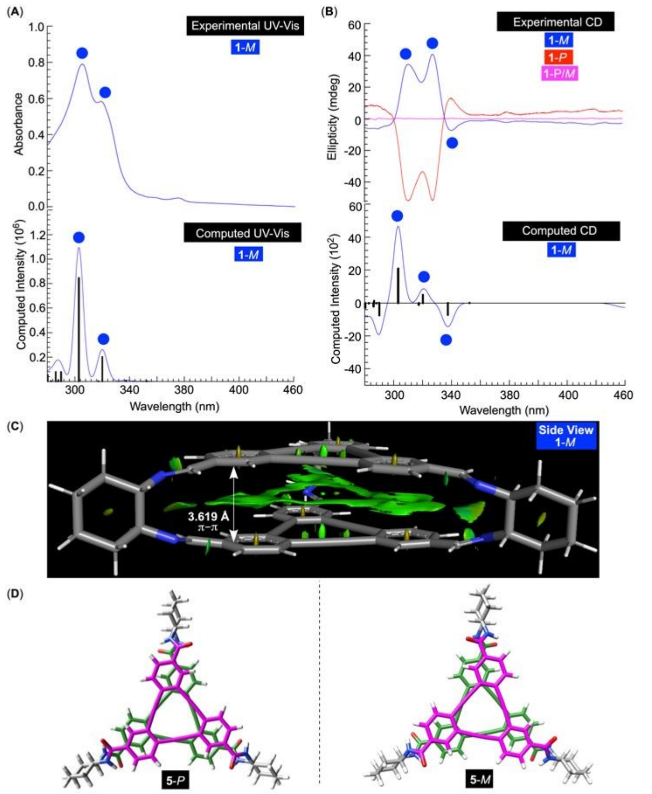

Fig. 4 (A) UV-Vis spectrum of **1**-*M* (40 μM in tetrahydrofuran) on top of its computed (DFT: B3LYP-D3/6-31+G* and TD-DFT: wB97XD/6-31+G*) electronic spectrum. (B) Circular dichroism (CD) spectra of **1**-*M* (40 μM in tetrahydrofuran), **1**-*P* (53 μM in tetrahydrofuran) and **1**-*P/M* (50 μM in tetrahydrofuran) on top of computed CD spectrum (DFT: B3LYP-D3/6-31+G* and TD-DFT: wB97XD/6-31+G*) of **1**-*M*. (C) Noncovalent interaction plot (NCI; Figure S29) of **1**-*M* (DFT: B3LYP-D3/6-31+G*) showing $\pi-\pi$ binding region (green gradient isosurface, PyMOL) between two DBA rings along with the centroid-to-centroid distance. (D) A stick representation of enantiomeric [2+3] amide cages **5**-*P* and **5**-*M* (OPLS4, Maestro).

In conclusion, we employed dynamic imine chemistry to incorporate two dehydrobenzo[12]annulenes (DBA) into [2+3] covalent organic cages. While aromatic systems comparable in size and shape to DBA assemble into [4+6] cages,[13, 19] here described and unexpected formation of [2+3] structures remains to be explained.[17] Moreover, the assembly occurs through a narcissistic self-sorting mechanism:[21] racemic *R* and *S*-CDAs react with DBAs to give two enantiomeric products in which three *R*-CDAs direct two DBA panels to assume *P* helical orientation and vice versa. In retrospect, the first successful incorporation of versatile dehydrobenzoannulenes[36] into discrete organic cages offers a potential for discovering novel catalytic,[37] optoelectronic,[23a] and storage[6a] materials about which we plan to report in the future.

Acknowledgements

This study was financially supported with funds obtained from the National Science Foundation under CHE-2304883. We thank Prof. Psaras McGrier and Jared G. Doremus (OSU) for assistance with examining Ni(0) coordination chemistry of DBA-based cages.

Conflicts of interest

There are no conflicts to declare.

Data availability

All research data reported here is available by e-mail from the corresponding author.

Notes and references

1. M. Mastalerz, *Acc. Chem. Res.*, 2018, **51**, 2411-2422.
2. S. J. Rowan, S. J. Cantrill, G. R. L. Cousins, J. K. M. Sanders and J. F. Stoddart, *Angew. Chem., Int. Ed.*, 2002, **41**, 899-952.
3. H. Ding, R. Chen and C. Wang, *Organic Cages through Dynamic Covalent Reactions*, 2018.
4. Z. Xu, Y. Ye, Y. Liu, H. Liu and S. Jiang, *Chem. Commun.*, 2024, **60**, 2261-2282.
5. M. Mastalerz, *Angew. Chem., Int. Ed.*, 2010, **49**, 5042-5053.
6. (a) T. Hasell and A. I. Cooper, *Nat. Rev. Mater.*, 2016, **1**, 16053; (b) S. Ro, S. J. Rowan, A. R. Pease, D. J. Cram and J. F. Stoddart, *Org. Lett.*, 2000, **2**, 2411-2414; (c) D. Xu and R. Warmuth, *J. Am. Chem. Soc.*, 2008, **130**, 7520-7521; (d) D. MacDowell and J. Nelson, *Tetrahedron Lett.*, 1988, **29**, 385-386; (e) J. Wu, Y. Wang, Z.-Y. Zhang and C. Li, *Chem. Eur. J.*, 2026, **32**, e03270.
7. (a) Y. Jin, B. A. Voss, R. D. Noble and W. Zhang, *Angew. Chem., Int. Ed.*, 2010, **49**, 6348-6351; (b) B. D. Egleston, K. V. Luzyanin, M. C. Brand, R. Clowes, M. E. Briggs, R. L. Greenaway and A. I. Cooper, *Angew. Chem., Int. Ed.*, 2020, **59**, 7362-7366; (c) K. Tian, W.-S. Zhang, A. K. Othayoth, M. P. Schuldt, F. Walenszus, F. Rominger, R. R. Schroeder, S. M. Elbert and M. Mastalerz, *Adv. Mater.*, 2026, **38**, e16358.
8. (a) Y. Zhang, M. Liu, Y. Wang and J.-H. Tang, *Chem. Commun.*, 2026, **62**, 1058-1069; (b) V. W. Liyana Gunawardana, C. Ward, H. Wang, J. H. Holbrook, E. R. Sekera, H. Cui, A. B. Hummon and J. D. Badjic, *Angew. Chem., Int. Ed.*, 2023, **62**, e202306722.
9. (a) H. Xie, T. J. Finnegan, V. W. Liyana Gunawardana, R. Z. Pavlovic, C. E. Moore and J. D. Badjic, *J. Am. Chem. Soc.*, 2021, **143**, 3874-3880; (b) H. Xie, T. J. Finnegan, V. W. Liyana Gunawardana, W. Xie, C. E. Moore and J. D. Badjic, *Chem. Commun.*,2022, **58**, 5992-5995.
10. (a) M. Shi, H. Yuan and W. D. Wang, *Chem. Commun.*, 2026, **62**, 2536-2553; (b) P. Bhandari and P. S. Mukherjee, *ACS Catal.*, 2023, **13**, 6126-6143.
11. (a) Z. Zhang, Y. Ying, Y. Li, M. Jin, S. Zhang, J. Wang, M. Yi, R. Chen, Q. Zhao, B. Li and X.-H. Bu, *Angew. Chem., Int. Ed.*, 2026, **65**, e22364; (b) S. Yu, J. Yang, Z. Song, Y. Su, Y. Guan and M. Liu, *Angew. Chem., Int. Ed.*, 2026, **65**, e20819; (c) T.

View Article Online
DOI: 10.1039/D6CC02397E

Hasell, M. Miklitz, A. Stephenson, M. A. Little, S. Y. Chong, R. Clowes, L. Chen, D. Holden, G. A. Tribello, K. E. Jelfs and A. I. Cooper, *J. Am. Chem. Soc.*, 2016, **138**, 1653-1659.

12. X. Liu and R. Warmuth, *J. Am. Chem. Soc.*, 2006, **128**, 14120-14127.
13. X. Wang, Y. Wang, H. Yang, H. Fang, R. Chen, Y. Sun, N. Zheng, K. Tan, X. Lu, Z. Tian and X. Cao, *Nat. Commun.*, 2016, **7**, 12469pp.
14. T. P. Moneypenny, A. Yang, N. P. Walter, T. J. Woods, D. L. Gray, Y. Zhang and J. S. Moore, *J. Am. Chem. Soc.*, 2018, **140**, 5825-5833.
15. (a) T. Tozawa, J. T. A. Jones, S. I. Swamy, S. Jiang, D. J. Adams, S. Shakespeare, R. Clowes, D. Bradshaw, T. Hasell, S. Y. Chong, C. Tang, S. Thompson, J. Parker, A. Trewin, J. Bacsa, A. M. Z. Slawin, A. Steiner and A. I. Cooper, *Nat. Mater.*, 2009, **8**, 973-978; (b) P. Skowronek and J. Gawronski, *Org. Lett.*, 2008, **10**, 4755-4758.
16. P. Kieryk, J. Janczak, J. Panek, M. Miklitz and J. Lisowski, *Org. Lett.*, 2016, **18**, 12-15.
17. K. E. Jelfs, E. G. B. Eden, J. L. Culshaw, S. Shakespeare, E. O. Pyzer-Knapp, H. P. G. Thompson, J. Bacsa, G. M. Day, D. J. Adams and A. I. Cooper, *J. Am. Chem. Soc.*, 2013, **135**, 9307-9310.
18. E. L. Spitler, C. A. Johnson, II and M. M. Haley, *Chem. Rev.*, 2006, **106**, 5344-5386.
19. H. Ding, Y. Yang, B. Li, F. Pan, G. Zhu, M. Zeller, D. Yuan and C. Wang, *Chem. Commun.*, 2015, **51**, 1976-1979.
20. X. Wang, P. Peng, W. Xuan, Y. Wang, Y. Zhuang, Z. Tian and X. Cao, *Org. Biomol. Chem.*, 2018, **16**, 34-37.
21. D. Beaudoin, F. Rominger and M. Mastalerz, *Angew. Chem., Int. Ed.*, 2017, **56**, 1244-1248.
22. G. Zhu, C. D. Hoffman, Y. Liu, S. Bhattacharyya, U. Tumuluri, M. L. Jue, Z. Wu, D. S. Sholl, S. Nair, C. W. Jones and R. P. Lively, *Chem. Eur. J.*, 2016, **22**, 10743-10747.
23. (a) Y. Lin, Y. Ge, C. Xu, H. Zhang, C. Cui, Y. Wu, L. Chi and Q. Chen, *J. Mater. Chem. C*, 2025, **13**, 15346-15353; (b) K. Tahara, T. Fujita, M. Sonoda, M. Shiro and Y. Tobe, *J. Am. Chem. Soc.*, 2008, **130**, 14339-14345.
24. W. K. Haug, E. R. Wolfson, B. T. Morman, C. M. Thomas and P. L. McGrier, *J. Am. Chem. Soc.*, 2020, **142**, 5521-5525.
25. E. R. Wolfson, N. Xiao, L. Schkeryantz, W. K. Haug, Y. Wu and P. L. McGrier, *Mol. Syst. Des. Eng.*, 2020, **5**, 97-101.
26. R. W. Hoffmann, *Chem. Rev.*, 1989, **89**, 1841-1860.
27. K. Matsumura, K. Kinjo, K. Tateno, K. Ono, Y. Tsuchido and H. Kawai, *J. Am. Chem. Soc.*, 2024, **146**, 21078-21088.
28. K. Hermann, Y. Pratumyot, S. Polen, A. M. Hardin, E. Dalkilic, A. Dastan and J. D. Badjic, *Chem. Eur. J.*, 2015, **21**, 3550-3555.
29. E. Gomez, M. Gutierrez, M. Moreno, I. Hisaki, S. Nakagawa and A. Douhal, *Phys. Chem. Chem. Phys.*, 2018, **20**, 7415-7427.
30. S. Stojanovic, D. A. Turner, A. I. Share, A. H. Flood, C. M. Hadad and J. D. Badjic, *Chem. Commun.*, 2012, **48**, 4429-4431.
31. S. Grimme, J. Antony, S. Ehrlich and H. Krieg, *J. Chem. Phys.*, 2010, **132**, 154104/154101-154104/154119.
32. (a) L.-J. Riwar, N. Trapp, B. Kuhn and F. Diederich, *Angew. Chem., Int. Ed.*, 2017, **56**, 11252-11257; (b) T. Lu, *J. Chem. Phys.*, 2024, **161**, 082503; (c) E. R. Johnson, S. Keinan, P. Mori-Sanchez, J. Contreras-Garcia, A. J. Cohen and W. Yang, *J. Am. Chem. Soc.*, 2010, **132**, 6498-6506.
33. P. J. Stephens, F. J. Devlin, C. F. Chabalowski and M. J. Frisch, *J. Phys. Chem.*, 1994, **98**, 11623-11627.
34. J.-D. Chai and M. Head-Gordon, *Phys. Chem. Chem. Phys.*, 2008, **10**, 6615-6620.
35. J. C. Lauer, A. S. Bhat, C. Barwig, N. Fritz, T. Kirschbaum, F. Rominger and M. Mastalerz, *Chem. Eur. J.*, 2022, **28**, e202201527.
36. S. Nobusue and Y. Tobe, *Advances in chemistry of dehydrobenzoannulenes*, 2015.
37. J. G. Doremus, B. Lotsi, C. A. Walker, A. N. Milligan and P. L. McGrier, *Energy Fuels*, 2024, **38**, 11356-11360.

View Article Online
DOI: 10.1039/D6CC02397E

Data availability

All research data reported here is available by e-mail from the corresponding author.